

Inelastic Collision Cross Sections at 1.0-, 4.0-, and 4.5-Mev Neutron Energies*

J. R. BEYSTER, R. L. HENKEL, R. A. NOBLES, AND J. M. KISTER
University of California, Los Alamos Scientific Laboratory, Los Alamos, New Mexico

(Received January 26, 1955)

Inelastic cross sections have been obtained from measurements of sphere transmission for incident neutron energies of 1.0, 4.0, and 4.5 Mev. Cross sections were measured for Al, Fe, Cu, Zn, Ag, Cd, Sn, Au, Pb, and Bi at the three neutron energies. In addition, the carbon inelastic cross section was measured at 1.0 Mev, the Be, C, Ti, Ni, Zr, and W cross sections were measured at 4.0 Mev, and the Ti, Ni, Zr, and W were measured at 4.5. The cross sections were determined at about ten energy thresholds of the neutron detector to obtain information about the energy spectra of inelastic neutrons. The experimental techniques and the method of evaluating the measurements are discussed. The results of this investigation are compared with other determinations of inelastic cross sections.

I. INTRODUCTION

THE measurement of inelastic collision cross sections for neutron energies in the Mev region has long been a difficult problem. A need for these cross sections arises in the study of neutron behavior in the core and shielding of nuclear reactors. Moreover, cross sections of this type are important for testing the validity of current nuclear models. From theoretical considerations on a specific model, the cross section for formation of the compound nucleus can be calculated.¹ The inelastic collision cross section is an experimental measure of this cross section if compound elastic scattering is negligible.

The cross sections to be discussed here were obtained from sphere transmission experiments. This method has been used extensively in the past.^{2,3} Part of the experimental results of this work have been published previously.⁴ In this paper the experimental procedures, numerical analysis, and all of the experimental results will be presented.

II. METHOD OF ANALYSIS

The sphere method of measuring inelastic collision cross sections has been discussed in detail elsewhere,^{5,6} and only a brief description and justification of the analytical procedures will be given here. The inelastic collision cross section is the sum of the cross sections for all processes except elastic scattering. The experimental arrangement for measuring sphere transmission

is shown schematically in Fig. 1. The sphere transmission in a constant neutron flux is the ratio of the counting rate with the sphere surrounding the detector to the counting rate with the sphere removed. To interpret this quantity in terms of the inelastic collision cross section the neutron source is considered to be at the sphere center in Fig. 1, with the detector outside the sphere at the original source position. The validity of this interchange of source and detector (reciprocity theorem) has been demonstrated elsewhere.⁵ The neutron multiple scattering analysis for spherical geometries proposed by Bethe^{5,6} is applied to specify the relationship between inelastic cross section and transmission. In this report, only neutrons which have no inelastic scatterings are considered. Two quantities P_n and \bar{P}_n ($n=0, 1, 2, 3, 4, \dots$) are now defined. P_n is the average probability that a neutron will escape from the spherical shell without another collision after having had n elastic collisions. \bar{P}_n is the average probability that a neutron will escape and be detected after having had n elastic collisions, divided by the probability of detection per source neutron when no sphere is present. Thus the transmission of a spherical shell is as follows:

$$T = \bar{P}_0 + (1 - P_0) \frac{\sigma_{el}}{\sigma_t} \bar{P}_1 + (1 - P_0)(1 - P_1) \left(\frac{\sigma_{el}}{\sigma_t} \right)^2 \bar{P}_2 + \dots, \quad (1)$$

where σ_{el} is the total elastic cross section and σ_t the total cross section. If N_0 is the number of atoms per cubic centimeter in the shell and r_1 and r_2 the inner and outer shell radii, respectively,

$$P_0 = \bar{P}_0 = e^{-N_0 \sigma_t (r_2 - r_1)}. \quad (2)$$

The general P_n is given by

$$P_n = \int_0^\pi \int_{r_1}^{r_2} N_n(r) dr \phi_n(\theta) d\omega e^{-N_0 \sigma Y} / \int_{r_1}^{r_2} N_n(r) dr, \quad (3)$$

* Work performed under the auspices of the U. S. Atomic Energy Commission.

¹ Feshbach, Porter, and Weisskopf, *Phys. Rev.* **96**, 448 (1954).

² Amaldi, Bocciarelli, Cacciapuoti, and Trabacchi, *Nuovo cimento* **3**, 203 (1946); C. H. Collie and J. H. E. Griffiths, *Proc. Roy. Soc. (London)* **A155**, 434 (1936); Szilard, Bernstein, Feld, and Ashkin, *Phys. Rev.* **73**, 1307 (1948); Gittings, Barschall, and Everhard, *Phys. Rev.* **75**, 1610 (1949); Phillips, Davis, and Graves, *Phys. Rev.* **88**, 600 (1952).

³ R. E. Carter and J. R. Beyster, *Phys. Rev.* **90**, 389 (1953).

⁴ Beyster, Henkel, and Nobles, *Phys. Rev.* **97**, 563 (1955).

⁵ H. A. Bethe, Report of Second Conference on Medium Energy Nuclear Physics at the University of Pittsburgh, 1953 (unpublished); H. A. Bethe, Los Alamos Report La-1428, 1952 (unpublished).

⁶ Bethe, Beyster, and Carter, Los Alamos Report LA-1429 (unpublished).

where σ is the cross section which determines whether the neutron makes another collision in the distance Y . The quantity $N_n(r)dr$ is the number of n th elastic collisions between r and $r+dr$. $\phi_n(\theta)d\omega$ is the probability normalized to unity of scattering elastically into solid angle $d\omega$ at angle θ on the n th elastic collision. Y is the distance through material a neutron must travel at polar angle θ from position r to escape from the sphere. \bar{P}_n is given by

$$\bar{P}_n = \frac{\int_0^\pi \int_{r_1}^{r_2} N_n(r) dr \phi_n(\theta) d\omega \frac{W(\alpha)}{\cos\alpha} e^{-N_0\sigma Y}}{\int_{r_1}^{r_2} N_n(r) dr}. \quad (4)$$

The $\cos\alpha$ occurs in this expression because of a geometrical effect which depends on the relative magnitudes of the sphere radius and the source to detector distance.⁵ The $W(\alpha)$ occurs because of the intensity and energy variation of the neutron source with angle.⁶ The determination of $W(\alpha)$ is discussed in Sec. III. The angle α in Fig. 1 is related to the independent variables in the above integral by the expression

$$\sin\alpha = (r/b) \sin\theta. \quad (5)$$

At this point three simplifying assumptions are made:

(1) The first assumption is that transport cross sections may be used to describe the second and later collisions in the shell (i.e., $\sigma = \sigma_{tr}$). The transport cross section is defined by

$$\sigma_{tr} = \sigma_{in} + \sigma_{el} \int_0^\pi 2\pi \sin\theta \phi_1(\theta) (1 - \cos\theta) d\theta,$$

where the right side of the equation is the sum of the inelastic collision cross section and the elastic transport cross section. P_1 and \bar{P}_1 may be calculated numerically now since $N_1(r)$ is $N_0\sigma_{el} \exp[-N_0\sigma_t(r-r_1)]$, $\phi_1(r)$ is proportional to the differential cross section for elastic scattering, and $W(\alpha)$ is available from experiment.

(2) The second assumption is that no significant errors will be made in computing P_n or \bar{P}_n ($n > 1$) if the asymptotic normal mode collision distribution for the shell [$N_m(r)dr$] is used. The escape probabilities calculated for Eqs. (3) and (4) by using the normal mode distribution are called P_m and \bar{P}_m , respectively. This assumption is justifiable for two reasons⁶: (a) The average escape probabilities do not depend markedly on the radial collision distribution, $N_n(r)dr$, used in the Eqs. (3) or (4). (b) The radial collision distributions converge quite rapidly with increasing n to the limiting distribution which is the normal mode. This approximation is most realistic for n large, but it gives reliable results even for P_2 and \bar{P}_2 . In the calculations for this report a slightly more accurate approximation to $N_2(r)dr$ than $N_m(r)dr$ is actually used.⁶

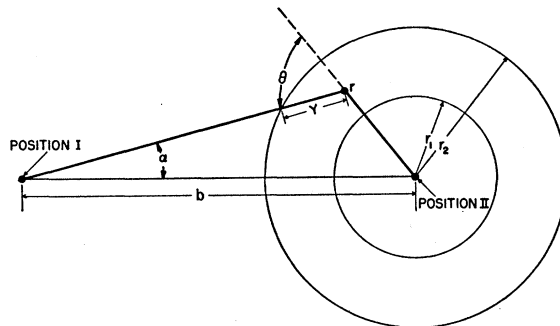


FIG. 1. Neutron source at Position I and neutron detector at Position II for the experimental measurements. These positions were reversed for the analysis of the measured transmissions.

(3) The third assumption made in the evaluation is that the quantities $\phi_2(\theta), \dots, \phi_n(\theta)$ are independent of θ , or that neutrons which have made second- or higher-order elastic transport collisions in the shell have their directions randomly oriented in space. All of the quantities needed to calculate P_2, \bar{P}_2, P_m , and \bar{P}_m are now available. Based on these considerations, Eq. (1) becomes

$$T = e^{-N_0\sigma_t(r_2-r_1)} + (1 - e^{-N_0\sigma_t(r_2-r_1)}) \left[\frac{\sigma_{el}}{\sigma_t} \left[\bar{P}_1 + (1 - P_1) \frac{\sigma_{et}}{\sigma_{tr}} \bar{P}_2 \right. \right. \\ \left. \left. + \frac{(1 - P_1)(1 - P_2)\sigma_{et}^2 \bar{P}_m}{\sigma_{tr}(\sigma_{in} + \sigma_{et}P_m)} \right] \right]. \quad (6)$$

The quantities σ_{et} and σ_{in} are the elastic transport and inelastic cross sections, respectively. Knowing three parameters [plus such auxiliary information as r_2, r_1, b , and $W(\alpha)$], one is able now to calculate the right side of Eq. (6). These parameters are the total neutron cross section σ_t , the shape of the elastic scattering angular distribution $\phi_1(\theta)d\omega$, and the inelastic collision cross section σ_{in} . A parametric study has shown that Eq. (6) is quite sensitive to the inelastic collision cross section for reasonably thin shells but not sensitive to the other parameters.⁶ Therefore one obtains the first two parameters from other sources of information and uses the observed sphere transmission to determine the inelastic cross section.

Equation (6) may be evaluated completely in a few seconds by a high-speed computing machine. It might therefore seem worthwhile to go a step further and to compute exactly the radial and angular distributions of neutrons that make second collisions or, for that matter, to treat all collisions exactly, using the Monte Carlo method. Many test cases⁶ have shown that this approximation [Eq. (6)] gives results in complete agreement with those obtained by the Monte Carlo method. In fact, for many problems it is not necessary to use a transmission equation as involved as Eq. (6),⁶ and the necessity of machine computing is thus eliminated.

Formulas previously presented assume a point de-

tector. The finite size of the detector used for these experiments is taken into consideration by the methods developed elsewhere.⁶ This effect is quite small for these detectors.

When a neutron is scattered elastically from a nucleus, its energy may be changed by only a small amount, but the sensitivity for detection may change considerably. This effect occurs for proton recoil counters biased to detect only neutrons close to the incident energy. The apparent increase in inelastic cross section produced by this effect can be estimated from the expression

$$\Delta\sigma = \sigma_{el}[1 - S(\bar{E})]. \quad (7)$$

\bar{E} is the average neutron energy after an elastic collision and $S(\bar{E})$ is the relative sensitivity for detecting this average energy neutron. To consider this effect as exactly as possible, the energy of a neutron while making elastic collisions in the shell is followed by the Monte Carlo method. On escaping from the shell, this neutron is placed in one of 46 energy groups. Each group is assigned an experimentally measured relative detection sensitivity. The observed shell transmission can now be corrected for this effect. If p_i is the relative probability of being in energy group i after escape and s_i is the relative detection sensitivity in this group, then

$$T_{obs} = T_{true} \sum_{i=1}^{46} p_i s_i. \quad (8)$$

It is necessary to process about 5000 neutrons to make this correction accurately in extreme cases.

To evaluate measured transmissions, the Bethe methods and the Monte Carlo method were combined and coded for the Los Alamos MANIAC computer. Inelastic collision cross sections are obtained as follows: For the input parameters T , σ_t , $\phi_1(\theta)$, r_1 , r_2 , etc., the computer calculates an apparent inelastic cross section by successive iterations using Eq. (6) plus a detector size correction term. It subtracts $\Delta\sigma$ [Eq. (7)] from this cross section to obtain an estimate of the true

inelastic collision cross section. This cross section, the total cross section, and the angular distribution for elastic scattering are introduced into the Monte Carlo problem. After the Monte Carlo analysis is completed, to remove the effect of losses of energy on elastic collisions, T_{true} [from Eq. (8)] is set equal to the right side of Eq. (6) with the addition of a detector size term. The inelastic collision cross section is determined from successive iterations in this modified equation. The entire problem for one element at one neutron energy with ten transmissions (measured at ten energy thresholds of the neutron detector) requires about an hour of computing time on the Los Alamos MANIAC.

III. EXPERIMENTAL PROCEDURES

A. General

The geometry for all of the sphere transmission experiments is shown in Fig. 1. A $T(p,n)He^3$ neutron source was used. The total spread in neutron energies from the tritium target was about 160 keV at 1 MeV and 70 keV at 4.0 and 4.5 MeV. The analyzed proton beam from the Los Alamos large electrostatic generator passed through an aluminum foil 0.0001 in. thick into a tritium gas target 6 cm long. The sphere and neutron detector were placed in the forward direction at about 30 in. from the source. A long counter⁷ was positioned at 120° from the forward direction and about 2 meters from the target. This counter and a precision current integrator were used independently for monitoring.

The neutron detectors were of the biased proton recoil type. Electronic-amplifying and pulse-height discrimination circuits had to be very stable because of the high biases (energy thresholds) used in the experiments. At these biases a fraction of a percent drift in the gain could change the counting rate several percent. Three carefully chosen amplifiers and preamplifiers were placed in parallel as indicated in Fig. 2. Pulses from these circuits were fed into a system of 15 discriminators and scalars. Ten energy thresholds were used; the remaining scaling circuits were placed in parallel on the selected biases. Scalars with the same bias used different amplifiers so that gain fluctuations in any counting channel could be detected while data were being taken. To check over-all gain stability directly, a signal from a precision pulser was applied at the preamplifier input and a counting-rate meter measured the output counting rate after the pulse-height discrimination stage in a scaler. When the pulse-height discrimination was adjusted so that a certain height of pulse applied at the preamplifiers would just trigger a discriminator, then a subsequent gain change in an amplifier or a change in the pulse-height discrimination level in the scaler could be easily detected. It was possible to detect and compensate for changes in gain or discrimination level of less than 0.05 percent. All of

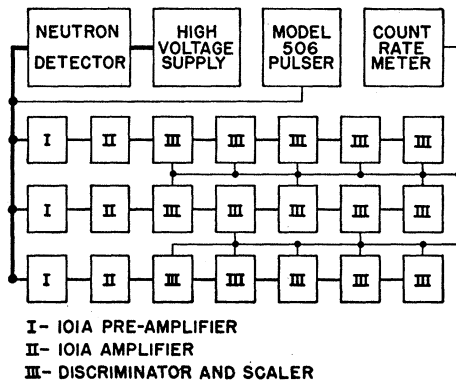


FIG. 2. Electronic arrangement used for the measurement of sphere transmission.

⁷ A. O. Hanson and J. L. McKibben, Phys. Rev. **72**, 673 (1947).

the amplifiers and scalers used 115-volt ac from regulated power supplies. Temperature control was maintained to about $\pm 1^\circ\text{C}$ on the amplifiers, preamplifiers, and seven of the scalers. These scalers were used on the most critical high biases. Gain drifts of less than 0.2 percent occurred in a normal day's operation.

Routine data taking consisted of measuring the sphere transmissions at least twice for a consistency check. Runs were arranged symmetrically (i.e., sphere off, sphere on, sphere off, sphere on, sphere off) to minimize any electronic gain or neutron yield drifts. The statistical error of a transmission measurement was about 0.4 percent at the higher biases, introducing usually less than 3 percent uncertainty in the final inelastic cross section.

B. 1-Mev Neutron Measurements

In the 1-Mev measurements the proton recoil proportional counter shown in Fig. 3 was used. The envelope of this counter was $\frac{1}{32}$ -in. thick brass and the collecting

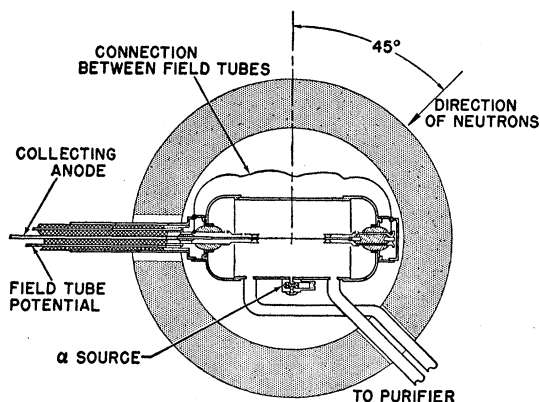


Fig. 3. Gas proportional counter for 1-Mev neutron measurements shown in position inside a sphere.

anode was a stainless steel wire 0.001 in. in diameter. At each end of the counter, field tubes⁸ surrounded the central wire so that the counting volume would be precisely determined. The gas filling was 20 percent methane and 80 percent krypton at a pressure of 100 psi. The gas was purified with magnesium ribbon at a temperature of about 160°C .

The characteristics of this detector of importance for the sphere experiment were investigated. The sensitivity of the detector to gamma rays was measured with known source strengths of Cs^{137} and ThC'' . This investigation showed that gamma rays from inelastic scattering in the sphere would not be detected significantly (less than 1 gamma-ray count per 1000 neutron counts). An asymmetric counter was undesirable since it would preferentially detect neutrons scattered into it from certain regions of the sphere. The angular

⁸ A. L. Cockroft and S. C. Curran, Rev. Sci. Instr. 22, 37 (1951).

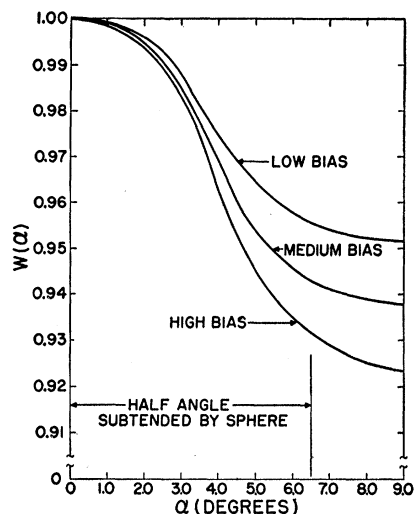


Fig. 4. Intensity versus angle for 1-Mev neutrons from $\text{T}(p,n)\text{He}^3$ neutron source.

asymmetry of the counter was investigated by rotating the counter, keeping its center at a fixed distance from the neutron source. When the gas multiplication was adjusted to be less than about five, the maximum asymmetry was less than 10 percent. To minimize the possible error due to this asymmetry, the counter was positioned as shown in Fig. 3. Counting losses were investigated by reducing the intensity of the neutron source by a factor of about ten and counting a correspondingly longer time, with no apparent change in the total counts recorded. The effect of room-scattered background neutrons was studied by measuring sphere transmissions, using a shadow cone to shield the direct neutrons from the counter. The magnitude of this background was less than 2 percent at the lowest bias and became negligible at the highest bias. Since sphere transmissions measured with the background flux were very nearly the same as those observed for the direct source neutrons, the effect was ignored.

The quantity $W(\alpha)$, used in Sec. II, was measured with the proportional counter at several angles smaller than 8° from the direction of the proton beam. Measurements were made at angles in both the horizontal and vertical planes. The counting rate relative to that at $\alpha=0.0^\circ$ was then plotted for each angle (α) and for each bias of the detector. Three of the measured curves of $W(\alpha)$ are shown in Fig. 4. The relative sensitivity of the detector to neutron energy $S(E)$ for the Monte Carlo calculations was measured by reducing the neutron energy in several steps of about 100 keV. The counting rate at each energy, divided by the rate at 1 Mev and adjusted for target yield changes with energy, is $S(E)$. The relative $\text{T}(p,n)\text{He}^3$ yields were measured with a long counter placed in the forward direction and agreed with the unpublished measurements of Jarvis *et al.* at this laboratory. Five of the

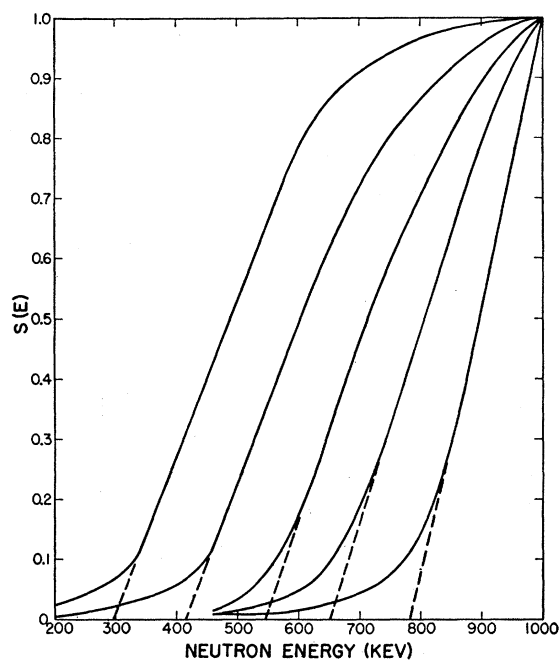


FIG. 5. Sensitivity *versus* neutron energy for biased gas proportional counter.

curves of $S(E)$ measured for this detector are given in Fig. 5.

C. 4.0- and 4.5-Mev Neutron Measurements

The recoil scintillation detector used in this experiment was similar to the counters designed and built by Bonner and co-workers⁹ to minimize gamma-ray sensitivity. The counter is shown in Fig. 6. Nine 0.100-inch diameter spheres were machined from a plastic phosphor, Pilot Chemicals Scintillator B. Each sphere was placed in a close-fitting hole ground into a quartz disk. These holes were located in three layers so that light from one phosphor emitted in the direction of the photomultiplier would not traverse another phosphor sphere. Optical contact between quartz and scintillator was obtained with Dow Corning 200 oil. The pulse-height distribution for monoenergetic 4.5-Mev neutrons in this detector, was not much different from that obtained from one plastic sphere. This indicated that there was nearly the same light-collecting efficiency from the various phosphor locations in the quartz assembly. At least 0.4 in. of clear quartz separated spheres in the assembly, eliminating the possibility of electrons with energy less than 5 Mev traversing any two spheres. It was possible, however, for an electron with an energy of about 800 kev to lose all of its energy in one phosphor sphere. The resulting pulse height would be equivalent to the maximum produced by a neutron of about 2.5 Mev. The gamma-ray sensitivity of the detector was measured for the various biases with sources of Cs^{137} and

⁹ McCrary, Taylor, and Bonner, Phys. Rev. 94, 808(A) (1954).

ThC'' of known activity. For the worst situation (2.4-Mev threshold), gamma rays produced by inelastic neutron scattering in the sphere produced less than 0.5 percent of the counts with the sphere on.

The background from the electrostatic generator and target assembly was investigated by filling the target with helium. For the lowest-energy threshold this background was about 1 percent. Sphere transmissions of this background were then measured and indicated that an error less than 0.3 percent in transmission might arise if no correction were made for this background. The effect of room-scattered background was again studied with sphere transmissions measured behind shadow cones. The magnitude of this background was also about 1 percent; neglecting it would cause an error less than 0.3 percent in transmission. A nuclear emulsion was exposed to the 4.0-Mev neutron source by L. Rosen of this laboratory, and showed that almost all of the neutrons above 2.5 Mev were in a single peak. The few percent that were not in this peak were in a continuous background spectrum. The measured transmissions at the low biases were not corrected for the above background and gamma-ray effects. These effects tend to cancel each other and neglecting them should result, at most, in an error of a few percent in cross section at the lowest bias.

The angular sensitivity of detector response was examined by the same methods mentioned for the 1-Mev experiment. The counter was uniformly sensitive at angles less than 150° , where the light pipe began to attenuate the neutron beam. Counter asymmetry was also investigated by measuring the transmission of a very thick ($2\frac{1}{2}$ in.) sphere of lead with the counter axis as shown in Fig. 6 and with the counter axis at 90° to this position. No difference in transmission outside of statistical counting errors (0.4 percent or less) was observed at any energy threshold of the neutron detector.

The effect of a magnetic material on the magnetically shielded Dumont photomultiplier was checked by replacing the neutron-sensitive detector with a NaI crystal at the end of the light pipe and placing a Cs^{137} gamma-ray source near this crystal. The crystal and source were then surrounded by an iron sphere and the position and shape of the photoelectric peak examined. No changes were observed.

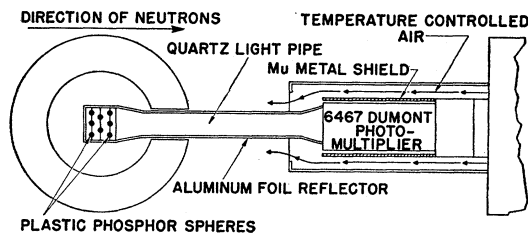


FIG. 6. Scintillation detector for 4.0- and 4.5-Mev neutron measurements shown in position inside a sphere.

To investigate the over-all effect of temperature on the light output of the crystal and on the photomultiplier tube gain, the detector shown in Fig. 6 was placed in an oven. These studies indicated that the over-all gain of this system changed by about 0.5 percent per degree centigrade change in temperature. This was a serious difficulty at the higher biases. Therefore the temperature controlled air system shown in Fig. 6 was installed.

Since the gain of the Dumont 6467 photomultiplier was very sensitive to tube high voltage, a precision potentiometer arrangement was used for monitoring and adjusting this voltage.

The quantities $W(\alpha)$ and $S(E)$ were measured by the methods discussed in the 1-Mev experimental section, Sec. III B.

IV. RESULTS AT 1 MEV

Inelastic cross sections measured at several energy thresholds of the neutron detector are given in Table I. The over-all rms errors in the 750-keV measurements are given. Smaller uncertainties are obtained at lower biases. The inelastic collision cross section for each element is also given in Table I. The best determination of this quantity is the measured inelastic cross section for the lowest-energy threshold at which a negligible number of inelastic neutrons are detected. The selection of this threshold is influenced by the available information on the energy levels of the target nuclei,¹⁰ and by the observed variations of inelastic cross section with energy threshold.

The uncertainties included in the determination of experimental error are: (1) the statistical uncertainty in the measurement of sphere transmission, (2) uncertainties in the measurements of $W(\alpha)$ and $S(E)$, (3) uncertainties in the parameters used in the multiple scattering analysis (σ_t and the angular distribution for elastic scattering), and (4) the uncertainty in the correction for loss of energy on elastic collisions. The total cross section and angular distribution parameters were obtained from 1-Mev elastic scattering angular

TABLE I. Inelastic cross sections for 1-Mev neutrons (barns).

Element	Inelastic collision cross section	Energy threshold (keV)					
		750	650	550	450	350	250
C	0.0 ± 0.04	-0.09 ± 0.14	-0.06	-0.03	-0.02	-0.01	0.00
Al	-0.01 ± 0.03	0.04 ± 0.08	0.04	0.03	0.01	0.00	-0.01
Fe	0.41 ± 0.03	0.41 ± 0.04	0.41	0.41	0.40	0.38	0.35
Cu	0.21 ± 0.04	0.21 ± 0.05	0.21	0.21	0.20	0.18	0.15
Zn	0.10 ± 0.06	0.10 ± 0.06	0.10	0.10	0.10	0.09	0.07
Ag	1.80 ± 0.20	1.61 ± 0.16	1.50	1.34	1.12	0.85	0.56
Cd	0.04 ± 0.08	0.99 ± 0.06	0.99	0.96	0.89	0.74	0.45
Sn	0.06 ± 0.05	0.07 ± 0.05	0.07	0.07	0.06	0.04	0.00
Au	1.80 ± 0.25	1.63 ± 0.10	1.46	1.26	1.05	0.79	0.54
Pb	0.21 ± 0.03	0.23 ± 0.04	0.23	0.22	0.21	0.19	0.16
Bi	0.12 ± 0.03	0.12 ± 0.04	0.12	0.12	0.12	0.12	0.12

¹⁰ Hollander, Perlman, and Seaborg, *Revs. Modern Phys.* **25**, 469 (1953); Way, Fuller, King, McGinnis, and Hankins, *Nuclear Data Cards* (National Research Council, Washington, D. C., 1955).

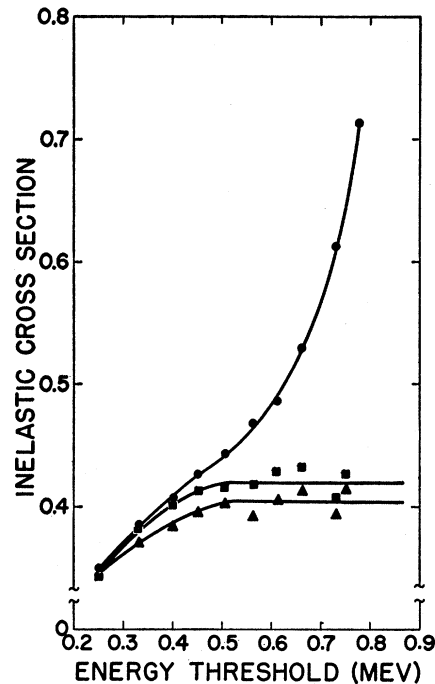


FIG. 7. Measured inelastic cross sections for iron at 1-Mev neutron energy. The circular points represent the cross sections before correcting for loss of energy in elastic collisions. The squares show cross sections calculated from the thin shell transmissions after correcting for loss of energy in elastic collisions. The triangles represent cross sections calculated from the thick iron shell transmissions after the energy loss correction.

distribution measurements.^{11,12} The fourth effect contributed most of the uncertainty in the cross sections given in Table I. By comparing the cross sections given in Fig. 7, it can be seen that the correction due to this effect is very large. If this correction had been made using the approximate method [Eq. (7)] instead of the Monte Carlo method, an additional uncertainty of as much as 10 percent would have occurred in the inelastic cross sections for the 750-keV bias.

Cross sections were measured as a function of energy threshold using two sphere thicknesses for iron and copper. Although the shell thicknesses differed by a factor of two, the calculated cross sections are the same within experimental errors, as shown for iron in Fig. 7.

The inelastic collision cross sections in Table I were compared with those given in reference 11 for elastic scattering angular distribution experiments. The uncertainties in the cross sections determined from those experiments were between five and ten times as large as the uncertainties given in Table I. The two methods agree however within quoted errors. Kiehn and Goodman¹³ have reported cross sections at 1 Mev for exciting gamma rays by inelastic neutron scattering in alumi-

¹¹ M. Walt and H. H. Barschall, *Phys. Rev.* **93**, 1062 (1954).

¹² The angular distribution of elastic scattering (ϕ_1) for aluminum at 1-Mev neutron energy was obtained from recent unpublished measurements by Walton, Allen, and Taschek.

¹³ R. M. Kiehn and C. Goodman, *Phys. Rev.* **95**, 989 (1954).

num, iron, lead, and bismuth. Considering the spread in neutron energies for the sphere experiments, the results of the two investigations agree to within experimental errors.

Measured inelastic collision cross sections should be equal to or less than calculated cross sections for formation of the compound nucleus. The measured inelastic cross sections in Table I are for the most part less than the theoretical cross sections computed using the complex square-well potential of Feshbach, Porter, and Weisskopf.¹ Exceptions to this are silver and gold, for which the measured cross sections are two to three times as large as the theoretical cross sections for formation of the compound nucleus. Possible explanations of this are discussed elsewhere.¹ It appears that rounding off the corners of the square-well potential used in the calculations will bring theory and experiment into better agreement.¹⁴

Inelastic cross sections in Table I were measured at several energy thresholds to test the over-all experimental method in known cases and to gain a qualitative idea of the neutron spectrum from inelastic collisions in other cases. Threshold energy is defined as that energy at which the straight-line portion of the sensitivity curve extrapolates to zero sensitivity (see Fig. 5). Ideally, the difference between the total inelastic collision cross section for neutrons of energy E_0 and the cross section obtained for an energy threshold E_T is the cross section for inelastic processes resulting in excitation of levels in the target nucleus below energy $E_0 - E_T$. This is only qualitatively true here, however, since the proportional counter does not have an ideal sensitivity response.

The threshold data in Table I may be used to obtain cross sections for exciting *known* energy levels below 1 Mev by inelastic neutron scattering. The uncertainties in the derived cross sections are large, however, primarily for two reasons: (1) In many cases small cross section changes have to be interpreted and these

TABLE II. Inelastic cross sections at 4.0-Mev neutron energy (barns).

Element	Inelastic collision cross section	Energy threshold (Mev)						Results of reference 16
		3.4	3.2	3.00	2.80	2.60	2.40	
Be	0.62 ± 0.03 ^a	0.62 ± 0.05	0.62	0.62	0.62	0.62	0.62	0.60 ± 0.10
C	0.04 ± 0.04 ^a	0.04 ± 0.08	0.04	0.03	0.04	0.04	0.04	0.08 ± 0.10
Al	0.75 ± 0.04	0.75 ± 0.05	0.75	0.75	0.74	0.71	0.68	0.70 ± 0.20
Ti	1.28 ± 0.07	1.28 ± 0.09	1.28	1.25	1.20	1.15	1.09	1.2 ± 0.20
Fe	1.42 ± 0.05	1.42 ± 0.07	1.42	1.41	1.36	1.30	1.22	1.5 ± 0.20
Ni	1.35 ± 0.10	1.35 ± 0.09	1.35	1.35	1.35	1.34	1.32	
Cu	1.60 ± 0.05	1.60 ± 0.07	1.60	1.60	1.58	1.53	1.47	
Zn	1.69 ± 0.06 ^a	1.69 ± 0.06	1.69	1.68	1.63	1.56	1.46	1.7 ± 0.20
Zr	1.56 ± 0.05	1.56 ± 0.07	1.56	1.56	1.56	1.54	1.50	1.8 ± 0.20
Ag	2.05 ± 0.10	2.05 ± 0.10	2.05	2.03	1.99	1.93	1.87	
Cd	2.05 ± 0.10	2.05 ± 0.10	2.03	2.02	2.01	1.96	1.86	2.10 ± 0.20
Sn	2.09 ± 0.07	2.09 ± 0.10	2.09	2.09	2.08	2.03	1.96	2.10 ± 0.20
W	2.60 ± 0.20	2.58 ± 0.20	2.55	2.50	2.42	2.36	2.28	2.40 ± 0.30
Au	2.75 ± 0.15	2.75 ± 0.12	2.75	2.72	2.67	2.62	2.57	2.7 ± 0.30
Pb	1.86 ± 0.10	1.84 ± 0.08	1.84	1.81	1.76	1.72	1.67	1.9 ± 0.30
Bi	1.98 ± 0.09	1.98 ± 0.10	1.98	1.98	1.97	1.92	1.85	2.2 ± 0.30

^a The neutron energy used in these experiments was 4.07 Mev.

¹⁴ C. E. Porter (private communication).

changes are uncertain to 30 percent or more. (2) The multiple scattering of the inelastic neutrons in the sphere must in general be considered. Thus knowledge of the inelastic collision cross sections and elastic scattering angular distributions at energies less than 1 Mev is required. This information must be estimated at present and is quite uncertain.

The cross sections measured for each element at the various thresholds will next be considered.

Carbon, as expected, has zero inelastic cross section within the experimental uncertainty at the thresholds indicated in Table I.

Aluminum appears to have a very small inelastic cross section at 1 Mev, in agreement with the findings of Kiehn and Goodman.¹³

Iron has nearly the same cross section at all biases. However, slightly lower cross sections were measured at the lowest biases. This effect is somewhat larger than experimental error and may be due to several causes. One such cause is that the neutrons produced in inelastic scattering processes in the iron sphere may count with low sensitivity at these biases. Therefore the cross sections measured for the higher energy thresholds are the best measure of the iron inelastic cross section.

Copper has a small inelastic cross section at 1 Mev as might be expected, since the lowest energy level reported in either stable isotope is at 0.96 Mev.¹⁰

Zinc has a very small inelastic collision cross section at 1-Mev neutron energy. There are energy levels, however, below 1 Mev in Zn⁶⁷ (a 4 percent abundant isotope)¹⁰ which could be excited by inelastic neutron scattering.

Silver has two stable isotopes, Ag¹⁰⁷ and Ag¹⁰⁹. The assignment of cross sections for exciting the known levels in these isotopes is somewhat ambiguous. This interpretation of the cross-section variations with threshold is based on four levels, with energies of 0.09, 0.31, 0.41, and 0.94 Mev. A consistent assignment of cross sections for exciting these states is 0.21, 0.45, 0.45, and 0.69 barn per silver atom, respectively. The 0.69-barn cross section is probably the most accurately determined quantity, and it is uncertain to about 0.30 barn.

Cadmium has several stable isotopes and many excited states below 1 Mev. There is, however, no indication from the present experiment of very much inelastic scattering to levels below about 350 kev. Furthermore, the observed variation of inelastic cross section with energy threshold is explained if one assumes that about 90 percent of the inelastic events excite a level at about 0.60 Mev in the target nucleus.

Tin also has many stable isotopes. One gamma ray with energy less than 1 Mev has been observed to accompany neutron inelastic scattering.¹⁰ The cross sections in Table I, however, indicate that very little inelastic scattering takes place to excited states with energy less than 1 Mev in the tin nucleus.

Gold has excited states reported at 0.077, 0.268,

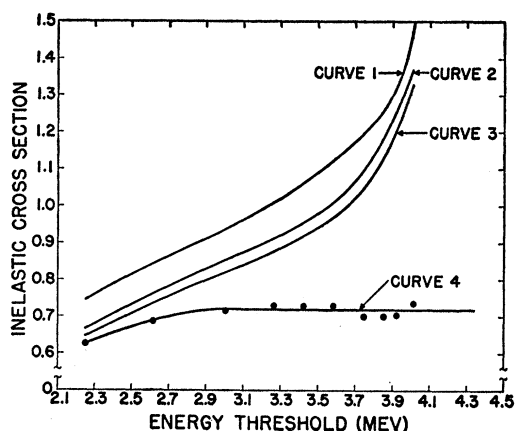


FIG. 8. Aluminum inelastic cross section at 4.5-Mev neutron energy. Curve 1 shows the cross section obtained from the exponential relationship {i.e., $T = \exp[-N_0\sigma_{in}(r_2 - r_1)]$ }. Curve 2 shows the cross section obtained after correcting for multiple neutron scattering in the shell. Curve 3 shows the cross section computed with corrections for multiple scattering and source intensity variation with angle. Curve 4 is drawn through the cross sections for the ten energy thresholds of the detector, and is computed with all of the corrections, namely, those of Curve 3 and the correction for loss of energy in elastic collisions.

0.279, 0.409,¹⁰ and 0.545 Mev.¹⁵ The general decrease in the cross section with threshold energy indicates that there is inelastic scattering to both low- and high-energy levels. A possible method of explaining these variations is to assign a 0.9-barn cross section to the excitation of the 545-kev level and 0.22, 0.45, and 0.23 barn, respectively, with the excitation of the 0.077-Mev level, the 0.268 and 0.279 levels taken together, and the 0.409 level. The uncertainty of each of these numbers is about 0.30 barn.

Lead has a measured inelastic cross section which varies slightly with energy threshold. This effect may be caused by inelastic collisions which excite the 0.55- and 0.89-Mev levels in Pb^{207} with a cross section of about 0.1 barn per lead atom.

Bismuth has a single stable isotope with its first excited state at 904 kev. No variation of inelastic cross section with energy threshold is indicated in Table I. One would expect the detection at low bias of the neutrons from inelastic scattering to produce a change in cross section of about 0.006 barn. The existence of this small change in cross section is very difficult to establish by the experimental methods employed here.

V. RESULTS AT 4.0 AND 4.5 MEV

Inelastic cross sections obtained at various energy thresholds of the detector for 4.0- and 4.5-Mev neutrons are given in Tables II and III, respectively. Experimental errors are placed on the data taken at a threshold of 85 percent of the incident neutron energy. The inelastic collision cross section for each element is

also given in the tables. This value is obtained from the measurement of inelastic cross section for the lowest energy threshold at which a negligible number of inelastic neutrons are detected. This threshold is chosen on the basis of information presently available on the energy levels in the target nucleus¹⁰ and on the basis of the observed behavior of the inelastic cross section with energy threshold. The sources of experimental error at 4.0 and 4.5 Mev are the same as those listed for the 1-Mev measurements. Total cross sections and elastic scattering angular distributions used in the numerical analysis are those measured recently at 4.1 Mev.¹⁶ The importance of various corrections applied to the data can be seen in Fig. 8. These results are based on the transmission measurements of an 8-in. diameter aluminum sphere at 4.5-Mev neutron energy. Figure 8 shows that even at this neutron energy the most important correction is that for loss of energy in elastic collisions. This is true also for heavy elements such as lead at 4.5-Mev neutron energy, for which a 12-percent correction must be made at the 3.8-Mev energy threshold.

The cross sections given in Table III at 4.5-Mev neutron energy for iron, copper, tin, cadmium, lead, and bismuth are based on transmission measurements for two shells differing by a factor of two in thickness. In all cases the two measurements agree to within the counting errors, suggesting that corrections are being made properly.

The energy thresholds of the neutron detector indicated in Tables II and III are obtained as at 1 Mev by extrapolating the sensitivity *versus* energy curves. Observed variations of cross sections as a function of threshold can only be considered a qualitative guide to which states of the target nucleus are being excited by inelastic events. Qualitatively then, one may say that 4.0- and 4.5-Mev neutrons will not excite low-lying levels in the target nucleus with high probability. In several cases it is possible to estimate the cross section for exciting known low-lying levels by inelastic scattering. The cross section changes observed at the various

TABLE III. Inelastic cross sections at 4.5-Mev neutron energy (barns).

Element	Inelastic collision cross sections	Energy threshold (MeV)							Results of reference 3
		3.80	3.60	3.38	3.15	2.93	2.70	2.48	
Al	0.72±0.04	0.72±0.06	0.72	0.72	0.72	0.72	0.70	0.67	0.82
Ti	1.18±0.07	1.18±0.09	1.18	1.18	1.16	1.13	1.10	1.04	
Fe	1.33±0.05	1.34±0.07	1.34	1.34	1.32	1.28	1.23	1.16	1.20
Ni	1.50±0.06	1.50±0.09	1.50	1.50	1.50	1.49	1.44	1.38	1.34
Cu	1.60±0.05	1.60±0.06	1.60	1.60	1.60	1.58	1.53	1.46	1.45
Zn	1.81±0.10	1.81±0.09	1.81	1.77	1.72	1.66	1.60	1.54	
Zr	1.59±0.07	1.59±0.09	1.59	1.59	1.58	1.58	1.56	1.52	1.64
Ag	2.02±0.10	2.02±0.11	2.02	2.02	2.01	1.97	1.92	1.84	2.01
Cd	2.12±0.12	2.12±0.11	2.11	2.10	2.07	2.05	1.99	1.92	2.11
Sn	2.18±0.06	2.18±0.10	2.18	2.18	2.17	2.13	2.09	2.02	2.05
W	2.60±0.20	2.56±0.20	2.56	2.56	2.56	2.52	2.45	2.38	2.68
Pu	2.70±0.15	2.69±0.13	2.69	2.69	2.69	2.67	2.63	2.58	2.62
Pb	2.02±0.14	2.02±0.16	2.02	2.02	2.02	2.00	1.97	1.93	2.19
Bi	2.19±0.08	2.19±0.10	2.19	2.19	2.19	2.17	2.14	2.09	2.32

¹⁵ W. I. Goldburg and R. M. Williamson, Phys. Rev. **95**, 767 (1954).

¹⁶ M. Walt and J. R. Beyster, Phys. Rev. **98**, 677 (1955).

energy thresholds of the detector are interpreted as in the 1-Mev analysis. In certain cases below it will be necessary to combine the cross sections for exciting two states because of a lack of sufficient energy resolution in the neutron detector. To increase the statistical accuracy of the calculation, the cross section for exciting a particular level is computed for both 4.0- and 4.5-Mev neutrons and the value given below is the average of these two numbers. The cross section for exciting the 0.84-Mev level, plus that for exciting the 1.02-Mev level in Al^{27} , is 0.19 ± 0.12 barn. The 840-kev level in Fe^{56} is excited with a cross section of 0.50 ± 0.20 barn by inelastic neutron scattering. The sum of the cross sections for exciting the 0.96-Mev level in Cu^{63} and the 1.12-Mev level in Cu^{65} is 0.49 ± 0.20 barn per copper atom. The 0.90-Mev level in Bi^{209} is excited with a cross section of 0.28 ± 0.15 barn by inelastic neutron scattering.

The 4.0-Mev cross sections are compared in Table II with those obtained from reference 16. The agreement between measurements done by the two methods is very good. In Table III the cross sections measured at 4.5 Mev are compared with those obtained from another sphere transmission experiment.³ A fission

neutron source and an $\text{Al}^{27}(n,p)\text{Mg}^{27}$ threshold detector were used in this experiment. The average neutron energy was 6 Mev and the half-width of the energy spectrum detected was about 3 Mev. This set of measurements is also in agreement with the present results.

Theoretical predictions of the cross section for formation of the compound nucleus have been carried out for 4.0-Mev neutron energy recently,¹⁶ using the complex square-well potential of Feshbach, Porter, and Weisskopf. The calculated cross sections are considerably lower than the observed inelastic cross sections given in Table II. This is the same difficulty which was observed for silver and gold at 1-Mev neutron energy.

ACKNOWLEDGMENTS

The authors gratefully acknowledge the considerable assistance of L. P. Grant and C. W. Johnstone with the electronic problems encountered in the experiments. We are also very much indebted to E. D. Cashwell and C. J. Everett for setting up the entire numerical computing problem for the Los Alamos MANIAC computer.

Spin, Quadrupole Moment, and Mass of Selenium-75*

L. C. AAMODT† AND P. C. FLETCHER
Columbia University, New York, New York

(Received January 27, 1955)

The microwave spectrum of OCSe^{75} has been observed and from it the spin, quadrupole moment, and mass of Se^{75} were measured. Frequencies of the six observed lines of the $J=2 \rightarrow 3$ rotational transition give a nuclear spin of $5/2$, a quadrupole coupling constant $eqQ=946.0$ Mc/sec, and a rotational constant $B_0=4081.926$ Mc/sec. From these and other known properties of the OCSe molecule, one obtains the quadrupole moment of Se^{75} as $Q=1.1 \times 10^{-24}$ cm² ± 20 percent, and the mass ratio $(M_{\text{Se}^{75}} - M_{\text{Se}^{76}})/(M_{\text{Se}^{75}} - M_{\text{Se}^{80}}) = 0.199566 \pm 0.000030$. The odd-even mass difference for Se^{75} is 1.5 ± 0.2 mMU. The observed spin disagrees with that expected from the shell model which predicts a spin of $1/2$ or $9/2$. Three possible nuclear configurations which agree with the observed spin and also indicate a positive quadrupole moment are $[\rho_{1/2}(g_{9/2})^2]_{5/2}$, $(g_{9/2})^2_{5/2}$, and $(f_{5/2})^2_{5/2}$. Magnetic moment measurements are needed to clearly distinguish between configurations. The sample material was obtained by bombarding arsenic with deuterons. Approximately $1\frac{1}{2}$ micrograms of sample material were produced but only 0.07 microgram could be used in each spectroscopic run because of difficulties in synthesizing OCSe .

INTRODUCTION

THE stable selenium isotopes Se^{74} , Se^{76} , Se^{77} , Se^{80} , and Se^{82} have sufficient natural abundance to make them available for microwave spectroscopy. Their nuclear properties have been determined or in the case of the even-even nuclei, confirmed by previous investigators.¹⁻³ Of the radioactive isotopes, Se^{79} , with

a half-life of 6.5×10^4 years, has had its nuclear properties determined by Hardy *et al.*⁴ Another selenium isotope which is amenable to microwave spectroscopy, because of a sufficiently long half-life (128 days⁵), is Se^{75} . Since this atom cannot be obtained with sufficient specific activity from pile bombardment to make measurements by microwave techniques possible, the sample material was produced by cyclotron bombardment. This is the first case where cyclotron bombard-

* Work supported by the U. S. Atomic Energy Commission.

† Now at Brigham Young University, Provo, Utah.

¹ Strandberg, Wentink, and Hill, Phys. Rev. **75**, 827 (1949).

² Geschwind, Minden, and Townes, Phys. Rev. **78**, 174 (1950).

³ W. Low, thesis, Columbia University, 1950 (unpublished).

⁴ W. A. Hardy *et al.*, Phys. Rev. **92**, 1532 (1953).

⁵ Cork, Rutledge, Branyan, Stoddard, and Le Blanc, Phys. Rev. **79**, 889 (1950).